Journal of Power Sources 189 (2009) 869–874

Contents lists available at ScienceDirect

Journal of Power Sources

journal homepage: www.elsevier.com/locate/jpowsour

Tailoring nanostructured TiO_2 for high power Li-ion batteries

B. Erjavec[a], R. Dominko[a,*], P. Umek[b], S. Sturm[b], A. Pintar[a], M. Gaberscek[a,c]

[a] National Institute of Chemistry, Hajdrihova 19, 1000 Ljubljana, Slovenia
[b] Institute of Jozef Stefan, Jamova 39, 1000 Ljubljana, Slovenia
[c] Faculty for Chemistry and Chemical Technology, Askerceva 6, 1000 Ljubljana, Slovenia

ARTICLE INFO

Article history:
Received 25 June 2008
Received in revised form 9 July 2008
Accepted 10 July 2008
Available online 25 July 2008

Keywords:
TiO_2
RuO_2
SiO_2
Rate performance
Li-ion batteries

ABSTRACT

It is shown that the rate performance of anatase TiO_2 can be significantly improved by addition of a small amount (few percent) of carefully selected oxides such as silica or RuO_2. Specifically, silica serves primarily as a suppressant of particle growth during heating of anatase precursor—in our case titania nanotubes. The addition of RuO_2 is supposed to enhance the electronic conductivity. The beneficial impact of the combined use of silica and RuO_2 in the preparation of anatase-based electrodes is also demonstrated on a commercially available sample of anatase.

1. Introduction

Unquestionably, energy storage is one of the greatest challenges in the modern society. Exploitation of renewable energy sources (photovoltaic, wind energy, braking energy, etc.) is credible if new power sources with both a high energy density and, simultaneously, a high power density are developed. One of the most serious candidates for such systems are lithium-ion batteries with their inherently high volumetric and gravimetric energy density and, possibly, also with a high power density provided that the electrodes are made of carefully designed nanostructured materials [1,2]. There are two ultimate aims of such nanostructurization: (a) a decrease of solid-state transport paths within the active particles and (b) optimization of the ionic and electronic wiring of the active particles [3,4]. Promising nanostructured materials for negative electrodes seem to be different polymorphs of TiO_2. It has namely been shown in several works that these materials, when used in the nanosized form, can accommodate up to 1 mol of lithium at moderate current densities between $C/10$ and $1C$ [5–7]. To achieve a good performance also at high current densities, the electronic and the ionic wiring have to be optimized as well. One way is to use porous materials with as high as possible surface area. The electrolyte-filled pores serve as conducting paths for ions. The access of electrons to the whole surface area is provided by decorating it with a thin layer of a semiconductor (e.g., amorphous carbon) or a metallic type of conductor (e.g., RuO_2) [8]. While the temperature needed for preparation of a semiconducting carbon layer is close to 700 °C [9], the temperature needed for preparation of RuO_2 is substantially lower. For example, RuO_2 with metallic conductivity can be prepared by a low temperature chemical vapour deposition [10,11] or by decomposition of $RuCl_3$ into RuO_2 in oxygen at 480 °C [12]. While the low temperature technique is rather complicated and expensive, the formation of RuO_2 from $RuCl_3$ is relatively simple and has been used for electronic wiring of mesoporous anatase [6]. The observed capacity is comparable to the one observed with a TiO_2-B polymorph [13], although the structure of the latter is more open and apparently better suited for fast kinetics. Two other papers have confirmed the importance of optimized nanoarchitecturing in order to achieve good high rate properties of anatase [14,15]. The best electrochemical results have been obtained in the case when 40 wt.% of carbon black was added to 6 nm large anatase particles [14]. Unfortunately, the authors do not explain the role of added carbon black. Our opinion is that it has a double role: it does not only provide the conductive paths for electrons but also serves as a spacer between the anatase particles thus allowing the electrolyte to wet all the active surface area (without such a spacer, the active particles would tend to agglomerate thus decreasing the effective surface area). This opinion is based on our recent preliminary study [16], in which we achieved similar results by carefully controlling the particle size as well as the wiring of the anatase particles. Specifically, we used thin silica (SiO_2) coatings to prevent TiO_2 particle growth during heat treat-

* Corresponding author. Tel.: +386 14760362; fax: +386 14760422.
E-mail address: Robert.Dominko@ki.si (R. Dominko).

0378-7753/$ – see front matter © 2008 Elsevier B.V. All rights reserved.
doi:10.1016/j.jpowsour.2008.07.030

ment. The heat treatment was necessary to prepare the RuO_2 phase which was supposed to provide electronic conductivity inside the electrode composite and to convert protonated titanium oxide nanotubes into anatase phase. Both additives, however, might also have served as spacers providing access of electrolyte (Li ions) to the anatase phase.

In the present contribution we show new results that additionally prove the beneficial impact of the combined use of silica and RuO_2. Furthermore, we extend our previous study, in which a model material was used, to a commercially available sample. Finally, we discuss in more detail the effect silica on the electrochemistry of the prepared composites.

2. Experimental

The preparation of protonated titanium nanotubes is explained elsewhere [16]. A part of the dried protonated titanum nanotubes was heat treated at 480 °C, the rest of the sample was used for the preparation of various TiO_2-based composites used in this study. The synthesis of SiO_2-coated titanium oxide nanotubes (TiO_2–SiO_2) was based on the use of TEOS (Aldrich, 98%) as the silicon source, with ammonia (Merck, 25%) as the catalyst and H_2O for hydrolysis. This mixture was kept at 40 °C in an ultrasound bath for an hour. After that, the mixture was left at 80 °C overnight to obtain a dry material. Finally, the material was thermally treated at 480 °C in air atmosphere. Another part of the sample was modified by $RuCl_3{\cdot}nH_2O$ (ACROS, 35–40% Ru) as a source of RuO_2 [6]. A mixture of 0.2 g of titanium oxide nanotubes and 20 mL of a 0.25 M solution of $RuCl_3{\cdot}nH_2O$ in absolute ethanol was treated in an ultrasound bath for 15 min. After that, the sample was vacuum filtered, dried in air and thermally treated under the same conditions as the composite described above. The obtained composites will be denoted as TiO_2/RuO_2. Finally, a fraction of the initial sample was prepared with both additives, SiO_2 (two different quantities) and RuO_2 (denoted as $TiO_2/SiO_2/RuO_2$). Firstly, we repeated the synthesis procedure with TEOS to obtain SiO_2 after the heating. Prior to thermal treatment, the dried material was immersed in an aqueous bath containing absolute ethanol and $RuCl_3{\cdot}nH_2O$. Then the same treatment was carried out as described above for the first two samples. In the same way we prepared four different composites (combinations of TiO_2, SiO_2 and RuO_2) using larger commercial anatase particles TiO_2-325 mesh (Aldrich, 248576) and low quantity of TEOS.

The surface morphology of the prepared composites was checked by field emission scanning electron microscope (FE-SEM SUPRA 35VP, Carl Zeiss). The morphology and composition of individual nanoparticles in the investigated composite were examined in a JEM-2010F 200 kV high-resolution (C_s = 0.5 mm) transmission and scanning electron microscope (TEM/STEM) equipped with an energy-dispersive X-ray (SiLi) detector. The X-ray powder diffraction patterns of the samples were collected on a PANalytical X'pert PRO MPD diffractometer using Cu $K\alpha_1$ radiation = 1.54056 Å in a reflection geometry. The data were collected in the range between 10° and 90° in steps of 0.034°.

The specific surface area, total pore volume and average pore width of materials examined in this study were determined from the adsorption and desorption isotherms of N_2 at 77 K using a Micromeritics ASAP 2020 instrument (model V3.01 H). This characterization was carried out after degassing of samples to 4 μm Hg for 30 min at 363 K and 2 h at 573 K. The specific areas of the samples were calculated by applying the BET method to the nitrogen adsorption data within the 0.06–0.30p/p^0 range. Pore size distributions were calculated from the desorption branch of the corresponding nitrogen isotherm, employing the BJH method.

Electrodes were prepared from the obtained composites, carbon black (AE 03972, Ketjen black) and polyvinylidenedifluoride (PVDF, Aldrich) binder in a weight ratio of 80:10:10. The slurry was prepared by thoroughly mixing an *N*-methyl-2-pyrrolidone (NMP, Merck) solution of PVDF, carbon black and the composite material. The mixed slurry was coated on a copper foil and dried in vacuum at 90 °C for 20 h. Coin-type electrodes (∅ = 8 mm) were cut out and used in cell assembly. The typical loading was 2 mg cm^{-2} of the composite ($TiO_2/SiO_2/RuO_2$) and the thickness of the electrode (without Cu substrate) was approximately 30 μm. Galvanostatic discharge/charge measurements were carried out using two-electrode coffee-bag cells with lithium metal as a counter electrode. The electrolyte used was a 1 M solution of $LiPF_6$ in EC:DEC (1:1 ratio by volume, all received from Aldrich). The working and the counter (lithium) electrodes were held apart with polypropylene/polyethylene separator (Celgard 2300 Microporous Membrane). The electrochemical characterisation was performed using a VPM3 Potentiostat/Galvanostat at room temperature at different current densities in the range from 335 mA g^{-1} (2*C*) to 80.4 A g^{-1} (480*C*). Here we use the conventional notation to allow comparison with previously published data [14]. All capacities are calculated based on the total mass of composite in the electrode (not just on the active mass of TiO_2).

3. Results and discussion

Due to their morphology (Fig. 1), protonated titania nanotubes are a good starting point for the synthesis of nano-sized active materials for Li-ion batteries [17]. As prepared titania nanotubes

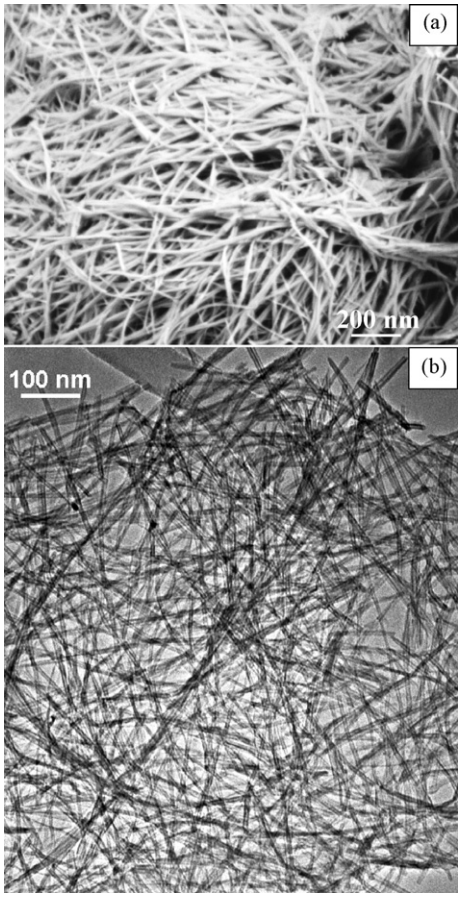

Fig. 1. (a) SEM and (b) TEM micrographs of as prepared protonated titanium oxide nanotubes.

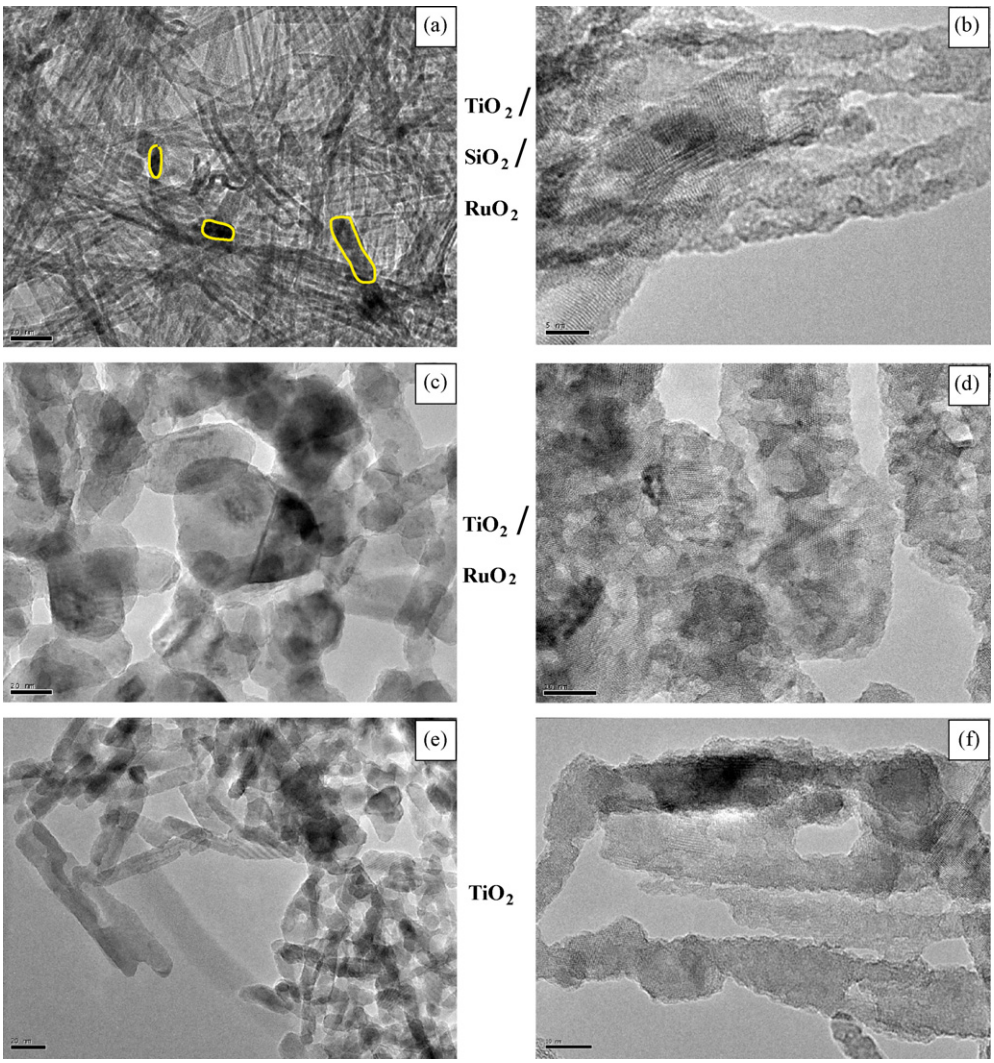

Fig. 2. TEM micrographs of: (a and b) $TiO_2/SiO_2/RuO_2$ composite, (c and d) TiO_2/RuO_2 composite and (e and f) TiO_2 composite. The left and the right micrographs were taken at different magnifications.

show poor electrochemical properties at high current densities [18] which, however, can be substantially improved by appropriate heat treatment during which the water is removed. The problem is that such a heat treatment not only removes the water but also leads to active particle growth and agglomeration. Recently, we have showed that particle growth can be suppressed, at least in the case of titanium oxide, by preparing very thin, and probably even discontinuous silica coating around titania nanoparticles. That simple idea led to interesting morphologies as displayed in Fig. 2. Fig. 2a and b present two TEM micrographs of a $TiO_2/SiO_2/RuO_2$ composite containing a low amount of silica. Comparing those figures with Fig. 1 it seems that the initial morphology of titanium nanotubes has not changed. However, at higher magnifications one can see that the nanotubes have actually re-crystallized into nano-sized crystals. A further analysis shows that the RuO_2 crystals appear as separate crystals (encircled particles in Fig. 2a). Their presence was confirmed using TEM-EDX and EELS spectroscopy analyses. Average TEM-EDX spectra obtained on the part of the sample where the presence of RuO_2 was not observed (RuO_2 particles crystallize in typical shape that is different to the TiO_2 crystals) are given in Fig. 3a. Any detection of the titanium phase was always accompanied by detection of silica; this suggests that silica must be distributed between or around the TiO_2 particles. If the TEM-EDX spectra were taken on the typical RuO_2 particles (encircled particles in Fig. 2a), then the major detected phase was RuO_2 (Fig. 3b). Finally, the TEM-EDX spectra taken on a larger area of the sample reveal the presence of all three phases (Fig. 3c). The two most evident features that follow from the TEM-EDX and TEM investigation of the $TiO_2/SiO_2/RuO_2$ composites can be formulated as follows: (a) the SiO_2 phase is distributed over the TiO_2 particles and (b) the RuO_2 phase is not percolating (this is important for understanding its actual role as an electronically conductive additive, see discussion below).

The morphologies of the samples prepared without the addition of silica precursor (Fig. 2c–f) are completely different than those observed when silica precursor had been used for preparation of the composite (Fig. 2a and b). The impact of silica precursor is clearly observed in TEM micrographs, which show significantly smaller TiO_2 (anatase) particles when silica is present. This demonstrates that silica indeed acts as a suppressant of particle growth. All X-ray diffraction patterns taken on the different TiO_2-based composites prepared in this study show that TiO_2 occurs in the form of anatase (Fig. 4). However, the width of Bragg reflections due to the anatase phase decreases systematically with the increased amount

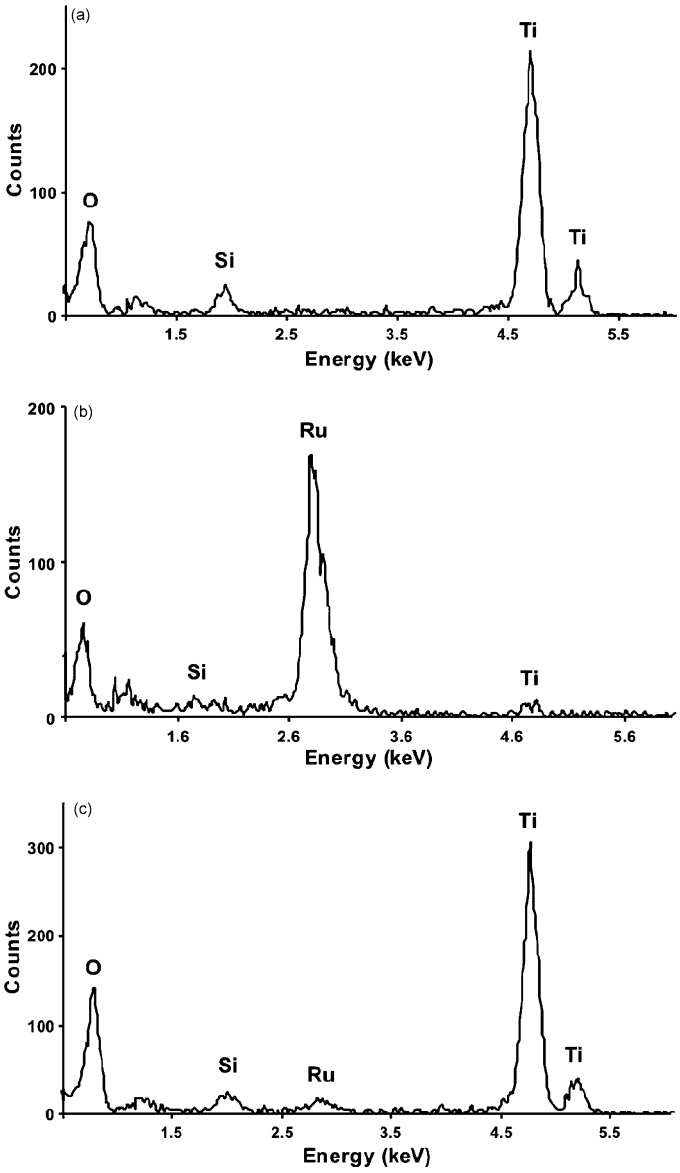

Fig. 3. (a) Average TEM EXD analysis of the $TiO_2/SiO_2/RuO_2$ composite, (b) TEM EXD analysis of RuO_2 particle and (c) TEM EXD analysis of TiO_2 particles.

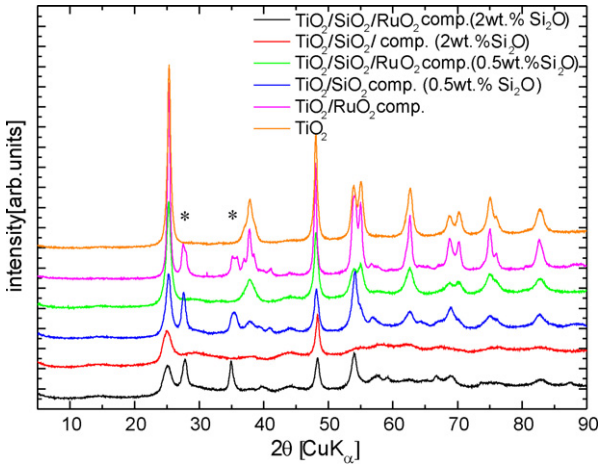

Fig. 4. X-ray diffraction patterns of five different combinations of composites based on two different quantities of silica in the composite.

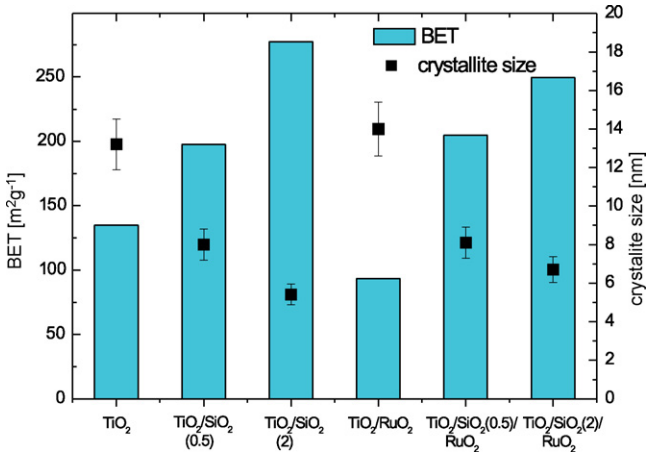

Fig. 5. BET surface area (left *y*-axis) and calculated crystallite size (right *y*-axis) as function of different combinations of composites based on two different quantities of silica in the composite.

of silica in the composite. This is a further confirmation that silica suppresses the growth of anatase phase. Interestingly, the width of Bragg reflections due to the RuO_2 phase (marked with asterisk) is very similar in all three composites containing RuO_2. This indicates that, most probably, that the RuO_2 particles are not interacting with silica. From the width of Bragg reflections the average crystallite size can be calculated using the Sherrer's formula. The average particle size is in good agreement with the BET surface area data (Fig. 5). The highest surface area (277 $m^2\ g^{-1}$) was obtained for the sample containing approximately 2 wt.% of SiO_2 in the composite for which the calculated crystallite size was 5.4 nm. The surface area of composites was substantially lower when a smaller amount (0.5 wt.%) of silica precursor was used, while the pure TiO_2 (anatase) sample shows a surface area of only 135 $m^2\ g^{-1}$ and a crystallite size of 13.2 nm. A similar trend in the BET surface area and the particles size was observed in the composites containing RuO_2. It is interesting, however, that the presence of RuO_2 slightly decreases the total BET surface area (compare the height of the first three and the second three columns in Fig. 5). Again, this decrease is consistent with the slight increase of the titania particle size when RuO_2 is added (see the squares in Fig. 5). Speaking naively, one could say that the presence of RuO_2 affects negatively the silica's role as a suppressant of the growth of titania nanoparticles. The effect, however, is small and certainly much less important than the general effect of silica.

The prepared composites possess significant porosity that is supposed to offer a good electrolyte penetration and thus a good ionic wiring—a precondition for a high power density electrode. Our electrochemical tests were focused to the current densities higher than 335 mA g^{-1} (>2*C* cycling rate). Fig. 6a shows charge/discharge curves obtained at a 2*C* rate. To avoid potential spurious effects in the first cycles, we show the electrochemical behaviour in the fifth cycle. All charge/discharge curves resemble those obtained previously for a nanoparticulate anatase phase [19]. The observed capacity is very similar for all four compared composites, however, it is obvious that the composites without silica are showing higher capacities in the region of lithium two-phase insertion (plateau region), while the composites coated with silica possess a higher capacity in the inclined region in which the surface charging is supposed to predominate [14]. The latter effect could be well explained by the decreased particle size (increased BET surface area) in silica-containing samples. It remains unclear, however, why silica affects the two-phase insertion region.

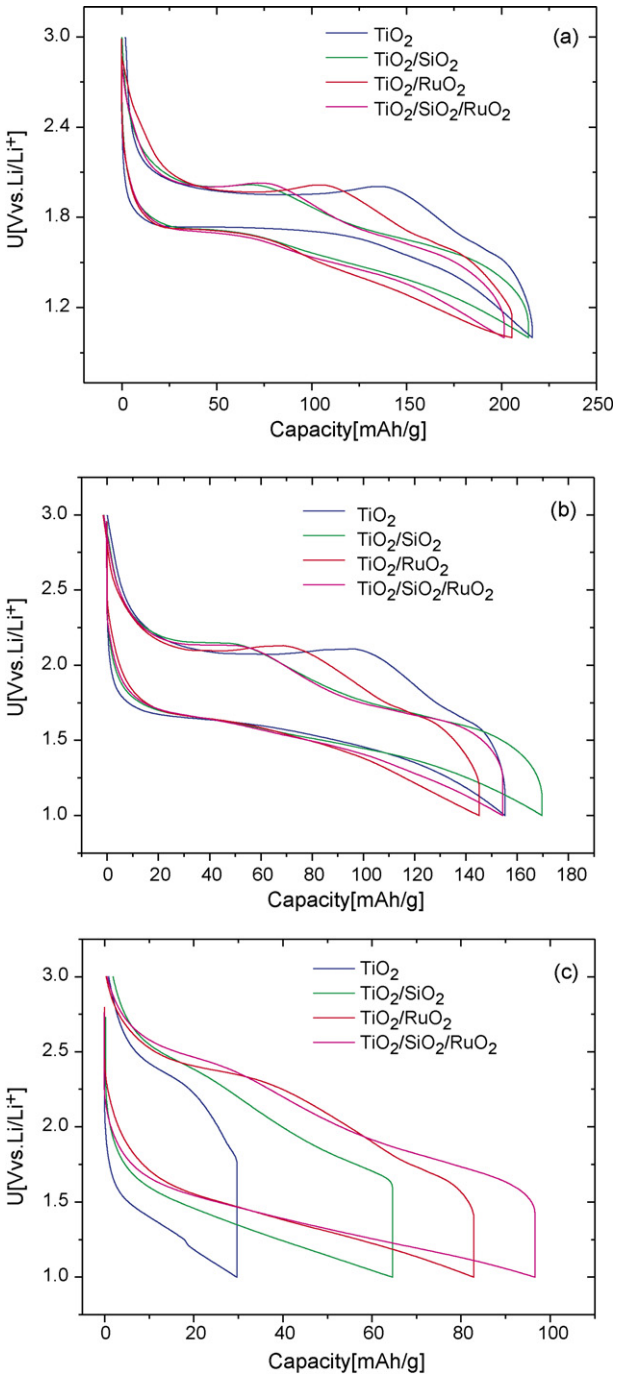

Fig. 6. Charge/discharge curves for different combinations of composites based on low quantity of silica at (a) 2*C* rate (335 mA g^{-1}), (b) 10*C* (1.675 A g^{-1}) and (c) 60*C* (10 A g^{-1}).

A similar electrochemical behaviour has been observed also in the charge/discharge curves obtained at a 10*C* cycling rate (1.675 A g^{-1}) only that the difference in the insertion mechanism is even more pronounced (Fig. 6b). The clearest is the picture at the highest rates of 60*C* (10 A g^{-1}, see Fig. 6c). The plateaus get very short in all cases if compared to the much longer inclined regions which are clearly correlated with the BET surface area—the higher the BET surface area the longer the inclined region. This is entirely consistent with the usual assumption that the slanted region is due to a supercapacitor-like behaviour of nanosized anatase. In fact, at high rates most of the capacity is due to supercapacitive rather than

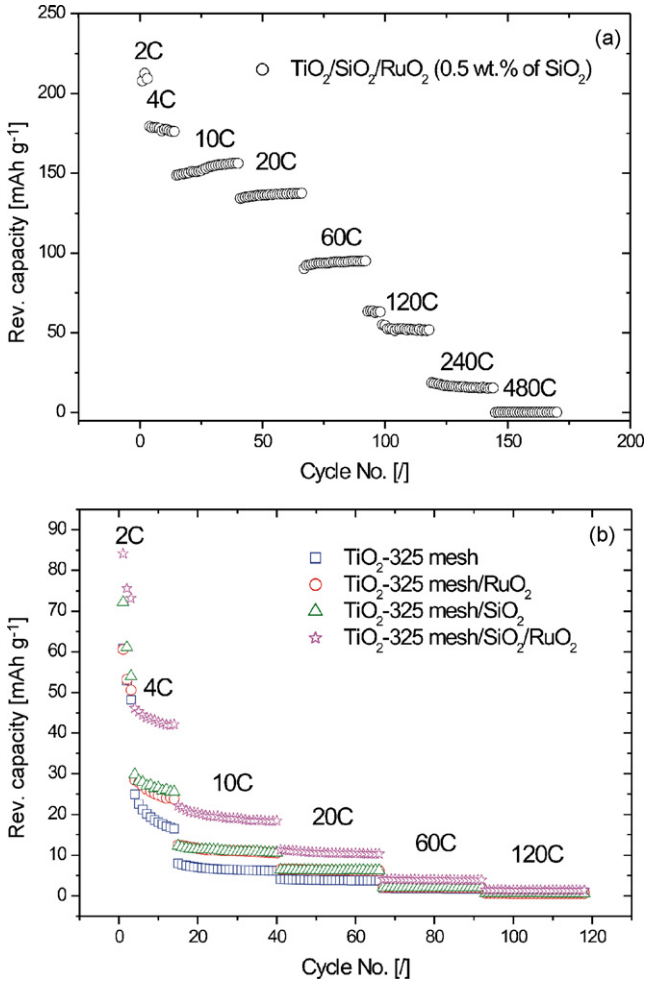

Fig. 7. Reversible capacity as a function of different current densities for (a) $TiO_2/SiO_2/RuO_2$ composite and (b) four different combinations of TiO_2-325 mesh-based composites prepared from commercial anatase.

insertion properties of anatase. It is known that a supercapacitor works well if the material has both a high surface area and if, at the same time, easy pathways for the charge leading towards the active surface are provided. One could speculate that silica certainly helps increase the total active surface area. Less clear is the role of RuO_2. Based on the previous works, we could assume that it serves as an additional medium that helps conduct the electrons [4]. In this particular case, however, such a role has still to be confirmed. What is obvious from Fig. 6c is that in the case when the electrode was made from pure TiO_2, the electrochemical response was the worst. As both silica and RuO_2 are beneficial for the capacity improvement it is not surprising that the highest capacity was observed when both additives were present in the composite.

To check the limiting conditions of operation of the $TiO_2/SiO_2/RuO_2$ composite, we have increased the current density up to 80 A g^{-1} (corresponding to a rate of 480 C). The obtained capacity (a few mA h g^{-1}) is then only displaying a sort of supercapacitor-like behaviour. By contrast, at lower current densities, such as 40 A g^{-1} (corresponding to a rate of 240*C*) or even lower, the $TiO_2/SiO_2/RuO_2$ composite shows a clear signature of lithium insertion into anatase phase (Fig. 7a).

To check whether the effect of silica and RuO2 additives can give improvement also with other anatase samples we have prepared a similar set of composites with commercial anatase particles obtained from Aldrich (Mesh#325). Fig. 7b shows the obtained

reversible capacities at different cycling rates for four different composites based on the commercial TiO_2-325 mesh anatase sample. As expected, the reversible capacities are now considerably lower due to the larger particles whereas at high cycling rates (60*C* and 120*C*) the reversible capacity is negligibly small. Interestingly, at moderate current densities (4*C*, 10*C* and 20*C*) the highest observed capacity is again for the composite containing both additives (RuO_2 and SiO_2). A significantly lower capacity was obtained for the composites where only RuO_2 and SiO_2 were added, however, the obtained capacity is still higher than in the case of pure TiO_2-325 mesh particles. This result confirms the beneficial effect of SiO_2 as an additive to the electrochemical performance of TiO_2. Further electrochemical tests and characterisation are required to elucidate the possible impact of SiO_2 as an additive, preferable also to other active materials.

4. Conclusions

Addition of a small amount (0.5–2 wt.%) of silica clearly prevents the growth of titania nanotubes upon heat treatment during which they are converted into anatase nanorods (or similar nanoshapes). For this reason, the resulting material exhibits much better rate performance if compared to the samples without addition of silica. A further enhancement of the anatase rate performance is obtained if, in addition to silica, precursors that during heating form RuO_2 are also added (again in a small amount of ca. 2 wt.%). The role of the latter additive is supposedly an enhancement of electronic conductivity, but this has still to be confirmed. A similar beneficial effect of both additives was obtained when the starting material were simply commercial anatase particles (rather than titania nanotubes).

Acknowledgements

The financial support from Slovenian Research Agency and the support from the European Network of Excellence 'ALISTORE' network are acknowledged.

References

[1] J.-M. Tarascon, M. Armand, Nature 414 (2001) 359.
[2] A.S. Arico, P. Bruce, B. Scrosati, J.-M. Tarascon, W. Van Schalkwijk, Nat. Mater. 4 (2005) 366.
[3] R. Dominko, M. Bele, J.M. Goupil, M. Gaberscek, D. Hanzel, I. Arcon, J. Jamnik, Chem. Mater. 19 (2007) 2960.
[4] Y.S. Hu, Y.G. Guo, R. Dominko, M. Gaberscek, J. Jamnik, J. Maier, Adv. Mater. 19 (2007) 1963.
[5] I. Exnar, L. Kavan, S.Y. Huang, M. Grätzel, J. Power Sources 68 (1997) 720.
[6] Y.-S. Hu, L. Kienle, Y.-G. Guo, J. Maier, Adv. Mater. 18 (2006) 1421.
[7] A.R. Armstrong, G. Armstrong, J. Canales, P.G. Bruce, Angew. Chem. Int. Edit. 43 (2004) 2286.
[8] J.B. Goodenough, Prog. Solid-State Chem. 5 (1971) 145.
[9] J. Moskon, R. Dominko, M. Gaberscek, R. Cerc-Korosec, J. Jamnik, J. Electrochem. Soc. 153 (2006) A1805.
[10] J. Sankar, T.K. Sham, R.J. Puddephatt, J. Mater. Chem. 9 (1999) p2439.
[11] J.V. Ryan, A.D. Berry, M.L. Anderson, J.W. Long, R.M. Stroud, V.M. Cepak, V.M. Browning, D.R. Rolison, C.I. Merzbacher, Nature 406 (2000) 169.
[12] Y. Murakami, T. Kondo, Y. Shimoda, H. Kaji, X.-G. Zhang, Y. Takasu, J. Alloys Compd. 261 (1997) 176.
[13] R. Armstrong, G. Armstrong, J. Canales, R. Garcia, P.G. Bruce, Adv. Mater. 17 (2005) 862.
[14] C. Jiang, M. Wei, Z. Qi, T. Kudo, I. Honma, H. Zhou, J. Power Sources 166 (2007) 239.
[15] M. Wagemaker, W.J.H. Borghols, F.M. Mulder, J. Am. Chem. Soc. 129 (2007) 4323.
[16] B. Erjavec, R. Dominko, P. Umek, S. Sturm, S. Pejovnik, M. Gaberscek, J. Jamnik, Electrochem. Commun. 10 (2008) 926.
[17] R. Dominko, E. Baudrin, P. Umek, D. Arcon, M. Gaberscek, J. Jamnik, Electrochem. Commun. 8 (2006) 673.
[18] J. Li, Z. Tang, Z. Zhang, Electrochem. Commun. 7 (2005) 62.
[19] G. Sudant, E. Baudrin, D. Larcher, J.-M. Tarascon, J. Mater. Chem. 15 (2005) 1263.